*Green Energy and Fuel Research*

Scilight

*Article*

Check for updates

# Comparative Energy Consumption and Indoor Airflow Analysis of Four HVAC Systems in an Office Building Using Revit-Based Modeling and CFD Simulation

Ivana Amelia Tamba [1], Chong-Kai Wang [2], and Yean-Der Kuan [2,3,4,*]

[1] Department of Refrigeration, Air Conditioning and Energy Engineering, National Chin-Yi University of Technology, Taichung 411, Taiwan
[2] Long Victory Instruments Co., LTD., Taoyuan 326, Taiwan
[3] Graduate Institute of Precision Manufacturing, National Chin-Yi University of Technology, Taichung 411, Taiwan
[4] Hydrogen and Fuel Cells Sustainable Development Center, Taichung 41170, Taiwan
* Correspondence: ydkuan@ncut.edu.tw
Received: 14 March 2026; Revised: 21 May 2026; Accepted: 26 May 2026; Published: 15 June 2026

**Abstract:** Improving energy efficiency in office buildings is key to achieving net-zero carbon emissions targets, particularly in hot and humid subtropical regions where cooling demand dominates. This study suggests an integrated framework that combines building information modeling (BIM), computational fluid mechanics (CFD), and energy simulation to evaluate the energy performance and indoor environmental conditions of various heating, ventilation, and air conditioning (HVAC) system configurations in an office building in Taiwan. An office building was created with Autodesk Revit. Annual energy simulations were carried out in accordance with ASHRAE Standard 90.1-2019. Four HVAC cases were analyzed, including variable air volume (VAV) with direct expansion (DX), VAV with a chiller, variable refrigerant flow (VRF), and a four-pipe fan coil unit (FCU) with a chiller. The energy performance of the four HVAC systems was evaluated using energy use intensity (EUI), together with CFD analysis of airflow and temperature distribution in the occupied zones. The comparison showed that the system configuration had a clear influence on overall performance. Case 2 produced the lowest EUI, with annual energy consumption 41.5% lower than that of Case 1, and its performance met the ASHRAE benchmark. Case 4 also showed favorable performance with high operational flexibility, while Case 3 showed intermediate efficiency. Case 1 demonstrated the highest energy consumption and lowest efficiency. CFD results under the prescribed boundary conditions indicate that the simulated occupied zones maintained acceptable temperature and airflow distributions. The findings show that chiller-based HVAC systems perform more effectively than DX-based systems in subtropical office buildings. The BIM–CFD–energy simulation framework developed in this study provides a useful basis for early-stage HVAC system comparison and selection, particularly for energy-efficient building design in high-cooling-demand climates.

**Keywords:** building information modeling (BIM); heating, ventilation, and air conditioning (HVAC); energy use intensity (EUI); flow simulation

## 1. Introduction

Energy use in buildings has become a major concern as countries work toward carbon reduction and net-zero targets. Although renewable energy is important, reducing the amount of energy buildings consume is still necessary to lower greenhouse gas emissions. The building sector accounts for roughly 30–40% of global energy consumption [1]. Among different building types, office buildings commonly have relatively high energy demand because they operate for long hours and contain dense occupancy, lighting, equipment, and other internal heat sources [2]. This issue is more pronounced in hot and humid regions such as Taiwan, where cooling is needed for much of the year and HVAC systems account for a large share of building electricity use [3]. For this reason, improving HVAC efficiency remains an important topic, and recent studies have examined passive and hybrid cooling strategies to reduce cooling demand and improve indoor environmental quality in office buildings [4–6].

BIM has gradually become an important tool for building performance studies because it can store both dimensional and spatial data, as well as non-structural data, within a single digital model [7]. Beyond design

visualization, BIM has evolved into a central data backbone for energy simulation and performance improvement [8]. Previous studies have shown that BIM-based energy simulation enhances visualization, improves the identification of spatial problems, and supports early detection of HVAC system malfunctions, thereby increasing the reliability of simulation inputs and results [9]. The integration of BIM and energy analysis tools, such as Autodesk Revit, enables evaluation of building energy performance during the early design stage. It also allows design parameters, including building orientation, envelope properties, construction materials, and mechanical system settings, to be examined before the building design is finalized. Previous BIM-based sustainability studies have reported that this type of workflow can assist in comparing different HVAC options and may help reduce EUI and lifecycle cost when the input data are properly defined [10,11]. However, the reliability of the simulation still depends strongly on the quality of the BIM data and on how well the information is transferred between the modeling and simulation platforms [12]. For BIM applications in building retrofits, incomplete information requirements, fragmented data organization, and limited interoperability have been identified as factors that can weaken the practical value of energy analysis results [13,14]. In addition, studies at the building design level have shown that orientation, envelope design, and climate-responsive parameters can significantly affect energy performance [15,16].

BIM has also been used alongside CFD simulations to support building energy performance evaluation. While energy models mainly describe whole-building or system-level performance, CFD provides more detailed information on airflow, temperature distribution, and heat transfer. These factors are closely related to HVAC operating efficiency and indoor thermal comfort. Autodesk CFD, which is based on fluid mechanics and heat transfer theory, can visualize airflow patterns and thermal behavior in more detail than conventional energy models. This is useful for buildings in dense urban areas, where surrounding structures, complex geometry, and local microclimate conditions can affect energy performance [17,18]. The combination of BIM and CFD is therefore useful for improving building energy analysis. By exporting detailed 3D models from Revit to Autodesk CFD, researchers can run repetitive simulations to examine airflow distribution, thermal stratification, and interactions between HVAC systems and indoor spaces. Kang et al. [19] reported that BIM–CFD integration can improve data interoperability and support "what-if" analysis for HVAC optimization. However, CFD simulation in buildings still depends strongly on boundary condition settings, treatment of heat accumulation, and model validation. Accurate calibration is therefore needed to obtain realistic results [20]. Recent studies have also stressed the need for CFD workflows that are experimentally guided, reproducible, and appropriate for complex indoor environments [21,22].

Occupant thermal comfort has also become an important issue beyond system-level airflow and temperature analysis. Previous studies on localized cooling and radiant-based systems have reported that indoor comfort can be improved without conditioning the whole indoor volume unnecessarily [23]. In non-uniform indoor environments, thermal comfort evaluation also needs to consider local physiological responses, radiant asymmetry, and spatial differences in thermal conditions, rather than treating the room as a uniform thermal space [24]. For this reason, HVAC evaluation in office buildings should include more than whole-building energy indicators. Airflow distribution, thermal stratification, and comfort conditions around occupants should also be examined.

EUI is widely used to assess building energy efficiency because it allows buildings with different sizes and functions to be compared on a common basis [25]. Earlier studies have shown that EUI is strongly influenced by the choice of HVAC system, envelope design, and operating strategy [26,27]. BIM-based energy modeling using Revit and Insight has demonstrated the potential to reduce energy use by over 50% in optimized scenarios [28] . Such results show that early-stage energy modeling might provide useful support for design decisions before the building configuration is finalized. BIM-based simulation can be applied not only to energy evaluation but also to the analysis of economic performance and lifecycle impacts. With cost assessment incorporated into the energy analysis process, different HVAC configurations can be assessed in terms of operating cost and practical feasibility. Studies that integrate real operational data from smart meters and sensors into building energy modeling (BEM) have improved the reliability of energy cost prediction and lifecycle assessment [29,30]. Recent work has also applied BIM to energy labeling, retrofit decision support, and lifecycle-based sustainability evaluation. Muta et al. [31] showed that BIM-based approaches can improve the accuracy and reliability of building energy labeling by integrating multiple evaluation methods into a single framework. Similarly, Kulthanaphanich et al. [32] developed a seven-module BIM framework for retrofit selection, quantitative analysis, energy assessment, seismic evaluation, lifecycle carbon and cost analysis, scheduling, and visualization. Their study showed that BIM can simplify data management and support multi-criteria evaluation in building retrofit projects. From a practical operations perspective, actual office-building energy optimization also needs to be evaluated in terms of technical feasibility, economic return, and environmental benefit rather than energy reduction alone [33].

This work compares four HVAC configurations for the same office building in Kaohsiung, Taiwan. The comparison was carried out using a Revit-based energy simulation model with the same building geometry,

operating schedule, and assessment conditions as in ASHRAE Standard 90.1 [34,35]. The four systems considered were VAV with DX cooling, VAV with an air-cooled chiller, VRF, and FCU with an air-cooled chiller. Rather than treating CFD as the primary tool for ranking a system's energy performance, this study uses CFD to assess whether the selected HVAC settings can provide acceptable indoor airflow and temperature distributions. In this way, the study provides a practical comparison of HVAC system options for office buildings in hot and humid subtropical climates.

## 2. Research Method

Figure 1 presents the research procedure used in this study. The office building was first developed as a three-dimensional BIM model in Autodesk Revit. After the model geometry was completed, the required simulation inputs were assigned, including envelope material properties, project location, weather data, operating schedule, and space zoning. The four HVAC system configurations were then created within the same Revit model to ensure that they were evaluated under consistent building and operating conditions. An annual energy simulation was conducted to determine the energy consumption, EUI, and operating cost for each case. The Revit model was also used as the basis for the CFD analysis, which examined the airflow and temperature distributions in the occupied zones. In this work, the CFD results were used to check the indoor environmental conditions rather than to determine the annual energy ranking of the HVAC systems. The energy simulation results and CFD analysis were then compared to evaluate the performance of the four HVAC configurations.

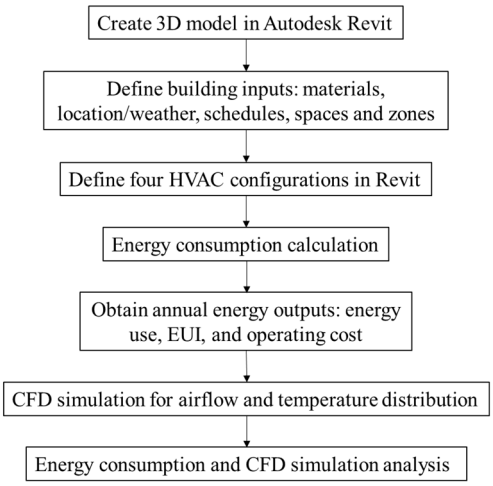


**Figure 1.** The workflow for the comparative evaluation of four HVAC systems.

### *2.1. Building Information*

In this study, the target building is located in Kaohsiung, Taiwan. The building consists of two floors and a rooftop, with a total floor area of 2165 $m^2$. The overall dimensions of the building are 45.5 m in length and 24 m in width. A three-dimensional model of the building was developed using Autodesk Revit, as shown in Figure 2. The spatial configurations of the first and second floors are illustrated in Figures 3 and 4, respectively.

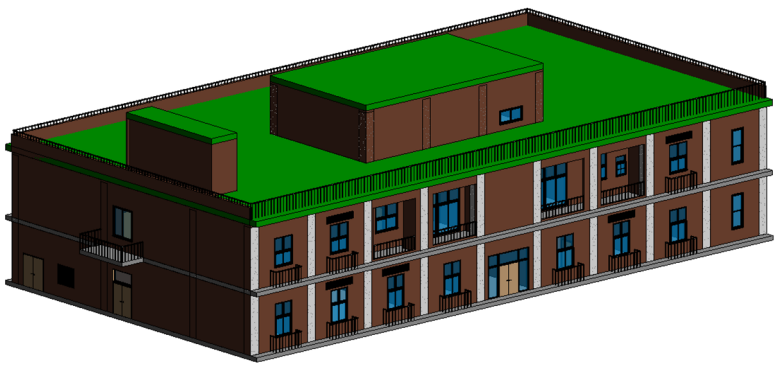

**Figure 2.** The building 3D model.

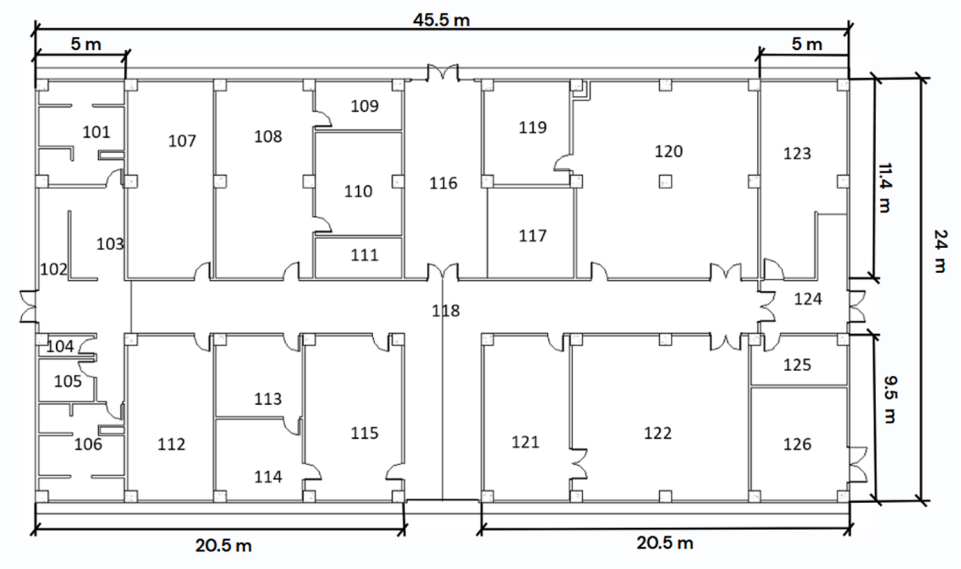


**Figure 3.** 1st floor plan of the studied building.

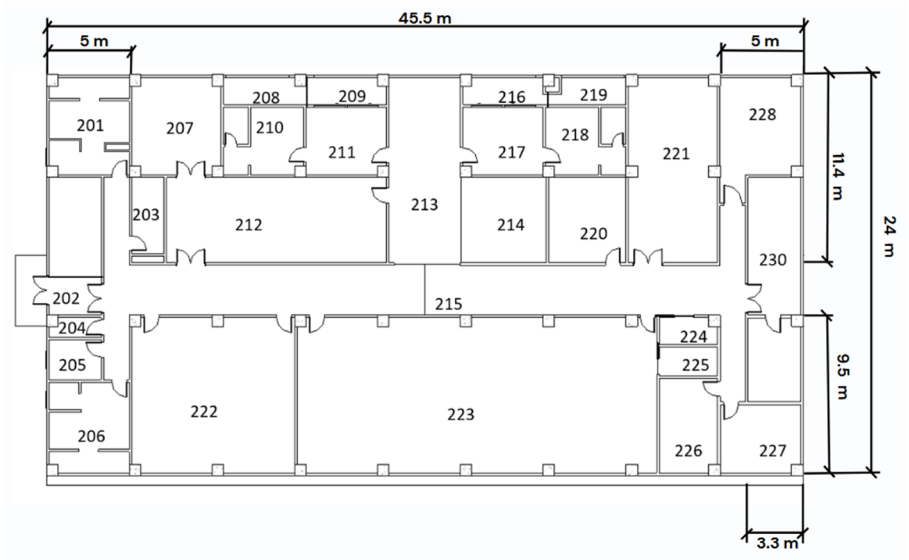


**Figure 4.** 2nd floor plan of the studied building.

Before comparing HVAC energy performance, the Revit energy model was set up with the required building and operation-related parameters. These included the thermal properties of the envelope, the project location, weather data, the operating schedule, the space function, and zoning information. Particular attention was given to the building envelope because windows and doors directly affect heat transfer through the building. For the windows, the glazing properties were specified using the U-factor, solar heat gain coefficient (SHGC), and visible transmittance (VT). Door settings were assigned based on their material makeup and insulation characteristics. The envelope-related parameters followed the requirements of ASHRAE Standard 90.1-2019. The project location in Revit was set to Kaohsiung, Taiwan, permitting the model to use the corresponding geographic coordinates, time zone, and local weather data. To represent a typical office-building operation, the office-building schematic type in Revit was selected. This setting provided default office assumptions for occupancy, internal loads, HVAC operation, and lighting. A 12-h-per-day, 5-day-per-week operating schedule was then applied to all simulation cases to compare the four HVAC systems under the same operating conditions. The main energy model settings are summarized in Table 1. The indoor spaces, including offices, toilets, stairs, and corridors, were first classified by function and then divided into conditioned and unconditioned areas. Conditioned areas were connected to the HVAC system for temperature control, while unconditioned areas were not provided with active heating or cooling. Based on this classification, the spaces were grouped into thermal zones, as listed in Table 2. Using the same zoning and scheduling assumptions across all cases allowed the comparison to focus on the effect of HVAC system configuration rather than on differences in building operation or space assignment.

**Table 1.** Energy simulation assumptions and input parameters.

| Parameter | Value |
|---|---|
| Thermostat setpoint | Cooling: 24–26 °C |
| Occupancy density | 0.1 person/$m^2$ (Revit automatic setting) |
| Lighting power density | 8.5–10 W/$m^2$ (Revit automatic setting by space type) |
| Equipment power density | 10–15 W/$m^2$ (Revit automatic setting by space type) |
| Weather data source | Revit data station (online automatic) |

**Table 2.** Classification of indoor spaces and building air-conditioning status.

| Floor | Function | Conditioned Status | Room Number |
|---|---|---|---|
| 1F | Office | Conditioned | 107−110,112–115,119–123,125,126 |
| | Toilet | Unconditioned | 101,104−106,111 |
| | Stairs | | 102,103,117,124 |
| | Corridor | | 116,118 |
| 2F | Office | Conditioned | 207,210–212,217,218,220,222,223,226–228 |
| | Toilet | Unconditioned | 201,203–206,224,225 |
| | Stairs | | 202,214,230 |
| | Corridor | | 213,215 |

### *2.2. Four HVAC Systems Evaluated in This Study*

To investigate the impact of HVAC system design on building energy consumption, four HVAC system configurations were implemented in the building model: VAV with DX, VAV with an air-cooled chiller, VRF, and FCU with an air-cooled chiller. The four cases are summarized in Table 3.

**Table 3.** HVAC systems and cooling types for each case.

| Case | HVAC System | Cooling Type |
|---|---|---|
| 1 | VAV | Direct expansion |
| 2 | | Air-cooled chiller |
| 3 | VRF | Refrigerant |
| 4 | FCU | Air-cooled chiller |

#### 2.2.1. VAV System with DX (Case 1)

Case 1 was designed as a centralized VAV system using direct expansion (DX) cooling for the studied office building. The system layout is presented in Figure 5. In this case, a central air handling unit (AHU) was equipped with a DX cooling coil and electric resistance heating. Conditioned air was supplied to different thermal zones through single-duct VAV terminal units. The airflow rate for each zone was controlled by terminal dampers according to the local zone demand. During part-load operation, electric reheat at the VAV terminals was used to maintain the required zone temperature. Since no chilled-water loop was included, the plant-side system was simpler than the chiller-based configurations.

For the energy model, Case 1 used the office-building settings in Autodesk Revit, including envelope properties defined by function parameters, no infiltration, and a 12/5 operating schedule. The DX cooling system was assigned a coefficient of performance (COP) of 5.96. Therefore, this case represents a typical refrigerant-based VAV system with centralized air handling and zone-level airflow control. It was used as the baseline case for comparing the other HVAC configurations in this study.

#### 2.2.2. VAV System with Air-Cooled Chiller (Case 2)

Case 2 was configured as a centralized VAV system using an air-cooled chiller as the cooling source. As shown in Figure 6, chilled water from the air-cooled chiller was supplied to a single AHU serving the office building under study. The AHU included a chilled-water cooling coil, a variable-volume supply fan, and an electric resistance heating coil. Conditioned air was delivered through four primary VAV terminal units, with two units assigned to the first floor and two to the second floor. Each primary terminal then supplied several sub-zones, allowing zone-level temperature control through a hierarchical zoning arrangement. Electric reheat was used at the VAV terminals when needed to prevent overcooling and maintain stable temperature control during part-load operation.

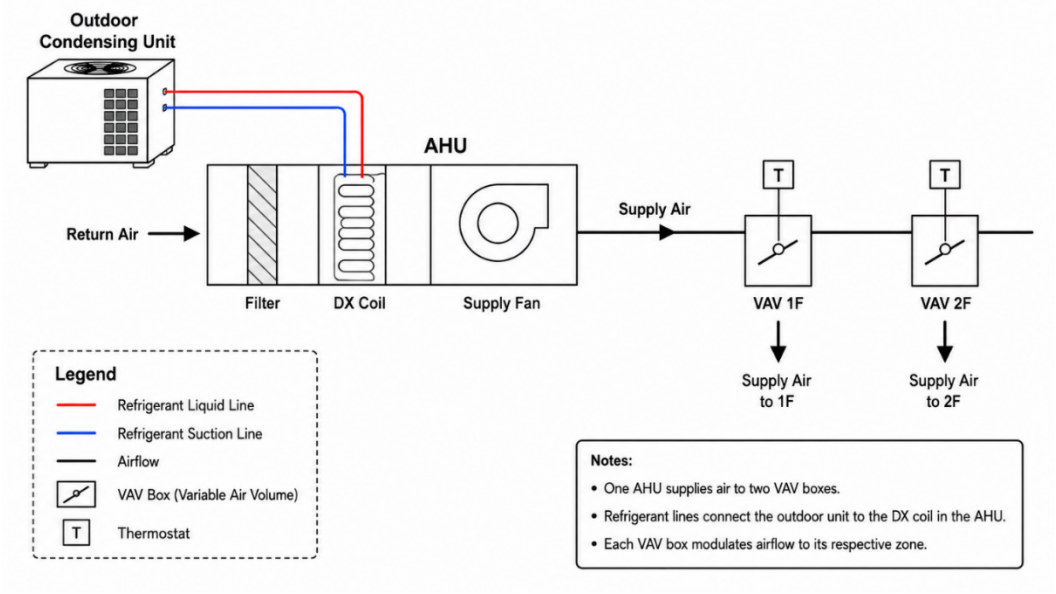


**Figure 5.** VAV direct expansion diagram.

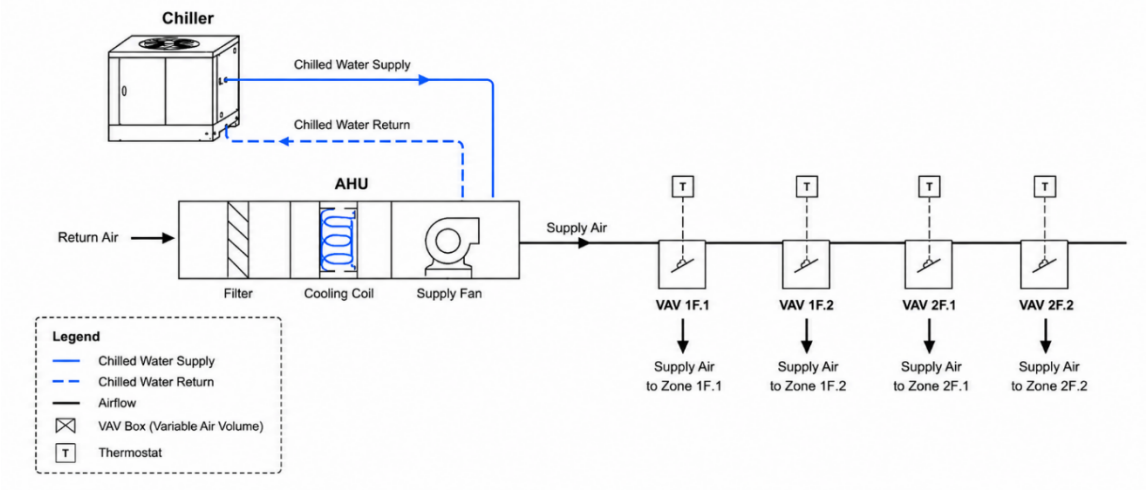


**Figure 6.** VAV air-cooled chiller diagram.

For the energy model, Case 2 used the same advanced energy settings as the VAV-DX case because both cases adopted the same VAV air-distribution arrangement. The office-type operating schedule and envelope-setting approach were therefore kept consistent. In this case, the DX cooling source was replaced by an air-cooled chiller, while the central AHU and VAV terminal layout remained unchanged. This setup made it possible to examine the effect of the cooling source on annual energy performance under comparable VAV operating conditions.

### 2.2.3. VRF System (Case 3)

Case 3 was modeled as a VRF system for the studied office building, with the system layout shown in Figure 7. In the simulation setup, the system consisted of 16 air-cooled CDUs, and each CDU was connected to one or two indoor fan coil units. This configuration formed a distributed refrigerant-based system for conditioning different thermal zones. Cooling was provided through direct refrigerant expansion with variable refrigerant flow control, while heating was supplied by heat pump operation under mild winter conditions. As chilled-water pumps and condenser-water equipment were not required, the system provided greater zoning flexibility and allowed decentralized conditioning at the room level.

For the energy model, the VRF case used envelope settings defined by function parameters, a 12/5 facility operating schedule, and no building infiltration. These settings were kept consistent with the other cases to evaluate the VRF system within the same office-building framework. Case 3, therefore, represents a distributed refrigerant-based HVAC option with zoning flexibility and part-load responsiveness. It was included to compare the performance of the VRF system with the more centralized VAV and chiller-based configurations.

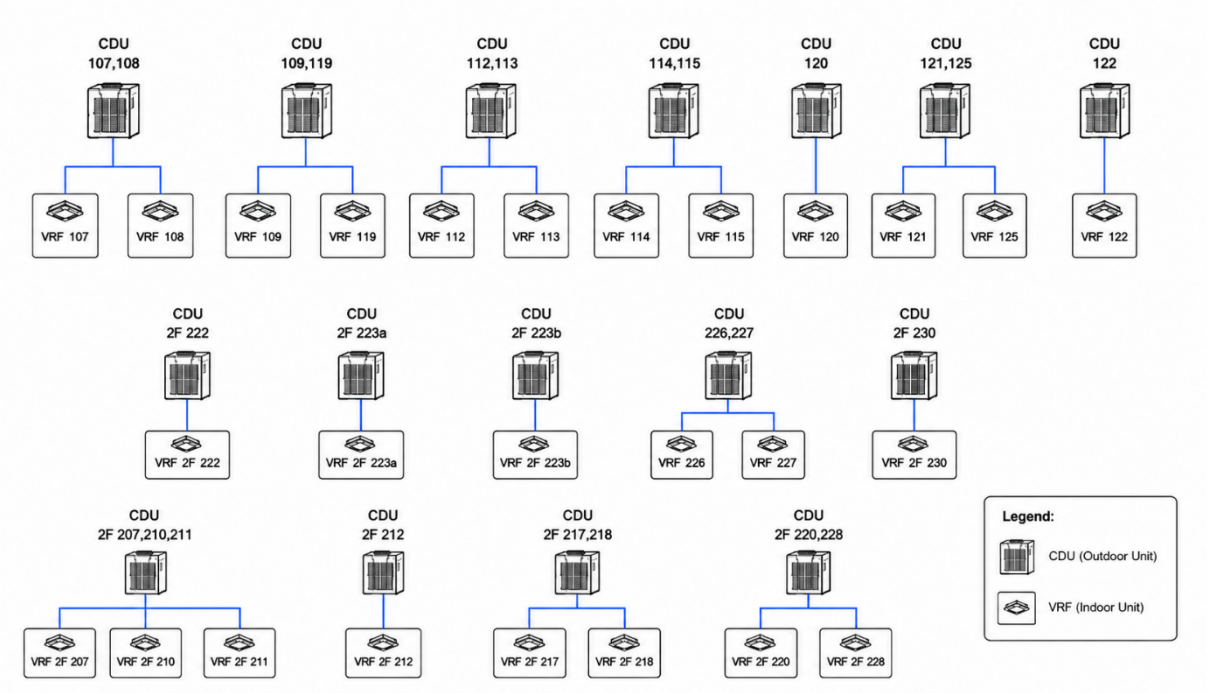


**Figure 7.** VRF diagram.

2.2.4. FCU with Air-Cooled Chiller System (Case 4)

Case 4 was configured as a centralized four-pipe FCU system for the studied office building. As shown in Figure 8, the system used an air-cooled chiller for chilled-water supply and boilers for hot-water supply. A total of 27 FCUs were distributed throughout the building. The chilled-water loop served the cooling coils, while a separate hot-water loop served the heating coils. Each FCU was assigned to an individual thermal zone, allowing cooling and heating to be provided in different zones according to local space demand. This four-pipe configuration allowed flexible zone-level control for multi-zone office operation.

For the energy model, the air-cooled chiller was assigned a COP of 5.96, and the boilers were assigned an efficiency of 84.5%. The model also used envelope properties defined by function parameters, no infiltration, and a 12/5 facility operating schedule. In the comparison of the four HVAC cases, Case 4 represents a water-based terminal-unit system with simultaneous heating and cooling capability. It was included to compare this type of system with the air-based VAV configurations and the refrigerant-based VRF system.

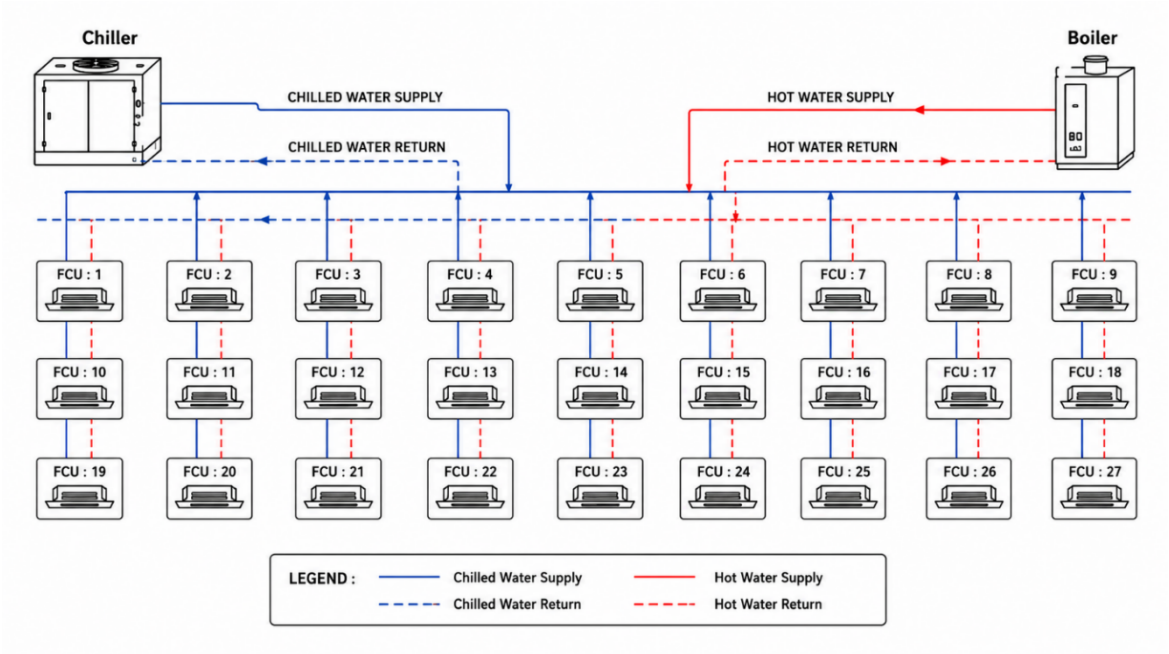


**Figure 8.** Centralized four-pipe FCU diagram.

### *2.3. CFD Simulation*

In Autodesk CFD, the simulation model was prepared by first assigning material properties to the main physical components. The building envelope surfaces were treated as concrete, with the material selected from the Autodesk CFD library and its thermal properties adjusted as required. The air region inside the model was defined as the computational domain, with air used as the working fluid under standard atmospheric conditions. Boundary conditions were then applied to the HVAC components to describe the supply and return airflow. At the contact surfaces between the concrete walls and the air domain, conjugate heat transfer was automatically generated by the software. The material interfaces were also checked to confirm proper connection, especially in areas where the airflow interacted with solid HVAC components.

The boundary conditions were set to describe the airflow and heat transfer behavior inside the model. At the diffuser surfaces, the supply air was modeled as a velocity inlet with an inlet velocity of 1.5 m/s, a supply temperature of 18 °C, and downward flow to represent conditioned air entering the space. The return grilles were assigned as pressure outlets, with an outlet pressure of 0 Pa and an upward flow direction to represent air extraction. Internal heat gains were added based on the load values calculated in the Revit model. The detailed boundary condition settings are listed in Table 4. The boundary conditions were applied as steady-state inputs, with fixed velocity and temperature values. To represent the thermal difference between spaces, conditioned and unconditioned zones were given different initial temperatures. The conditioned zones were set at 25 °C, which corresponds to the indoor comfort temperature maintained by the HVAC system. The unconditioned zones were initialized at 30 °C to represent spaces without active cooling. Because the conditioned and unconditioned zones were initialized with a 5 °C temperature difference, a thermal gradient was formed between adjacent spaces. This gradient affected heat transfer, airflow exchange, and convective heat migration across the shared boundaries. Once the geometry, material properties, and boundary conditions were set, the solver was configured to account for airflow, heat transfer, and gravity. The simulation was allowed to run until the residuals decreased and the monitor plots showed stable behavior.

**Table 4.** Boundary condition setup parameters.

| Boundary Condition | Type | Value |
|---|---|---|
| Diffuser | Velocity | Velocity: 1.5 m/s; Temperature: 18 °C |
| Grille | Pressure | Pressure: 0 Pa |
| Electricity | Load | Load density: 11.84 W/m$^2$ |
| Occupant | People | Sensible heat: 73.27 W, Latent heat: 58.61 W |

## 3. Results and Discussion

### *3.1. Energy Consumption of Various HVAC Systems*

This section presents the energy consumption results for the four HVAC system configurations. The building was modeled in Autodesk Revit, and the model was linked with energy simulation to estimate energy performance based on the defined building parameters. The following subsections discuss the energy results of each HVAC case in detail.

#### 3.1.1. VAV with DX System (Case 1)

Figure 9 shows the annual energy consumption of the VAV system with DX cooling. Because Kaohsiung has a humid subtropical climate, with an average annual temperature of about 24 °C and a long hot season, the building load is mainly cooling dominated. This trend is also reflected in the simulation results for the VAV-DX case.

In the simulation, the system was modeled with a single AHU that included a DX cooling coil, an electric resistance heating coil, and a variable-volume supply fan. The conditioned air was distributed to the first and second floors by two VAV terminal units. During part-load operation, electric reheat at the terminals was used to regulate the temperature of each zone. Although this arrangement allows zone-level control, it also increases reheat energy use when cooling and reheating occur at the same time. The annual results indicate that cooling was the largest energy end use, reaching 164,403 kWh. Fan energy was the second largest component, at 35,156 kWh, mainly due to air distribution through the ductwork and between floors. Heating energy was 16,900 kWh per year and was mostly related to electric reheat at the VAV terminals. Although the heating requirement is not large in Kaohsiung's climate, the use of electric resistance reheat still reduces the overall system efficiency. The annual energy consumption of office equipment and interior lighting was 38,883 kWh and 28,706 kWh, respectively, and both contributed to the internal cooling load. In contrast, pumps, heat rejection, humidification, and refrigeration showed no energy

consumption. This result is consistent with the DX-based configuration, as the system does not include a water loop or cooling tower.

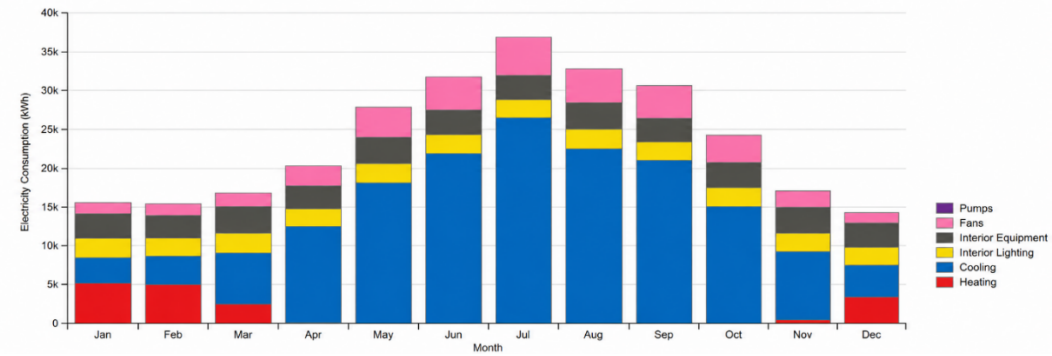


**Figure 9.** Annual energy consumption of Case 1.

### 3.1.2. VAV with Air-Cooled Chiller System (Case 2)

For Case 2, an annual energy simulation was conducted for a VAV system with an air-cooled chiller as the cooling source. The system included one AHU with a chilled-water cooling coil, an electric resistance heating coil, and a variable-volume supply fan. Conditioned air was supplied to both floors through four VAV terminal units, with two units serving each floor. The energy consumption results for this case are shown in Figure 10. The annual cooling energy was 66,792 kWh, much lower than in the VAV-DX case. This difference indicates that chilled-water cooling performed more efficiently for the studied cooling-dominated building. Fan energy and pump energy were 13,583 kWh and 3292 kWh, respectively. Although the chiller-based system required additional pump operation, the pump energy remained small compared with the reduction in cooling energy. Heating energy was 14,850 kWh per year, primarily due to the continued use of electric reheat at the VAV terminals during part-load operation. Office equipment and interior lighting consumed 38,883 kWh and 28,706 kWh per year, respectively, and these internal loads also increased the cooling requirement. The monthly electricity use followed the seasonal pattern of Kaohsiung's subtropical climate. The cooling load was highest in July, reaching 10,271.14 kWh. Heating demand occurred mainly in winter, with January and December showing relatively higher values. Lighting and office equipment, however, showed little monthly variation. Total electricity use ranged from 11,776.01 kWh in March to 17,912.57 kWh in July, giving an annual consumption of 166,105.56 kWh. Overall, the chilled-water VAV system used less energy than the VAV-DX system, primarily due to its improved cooling efficiency and more stable temperature control.

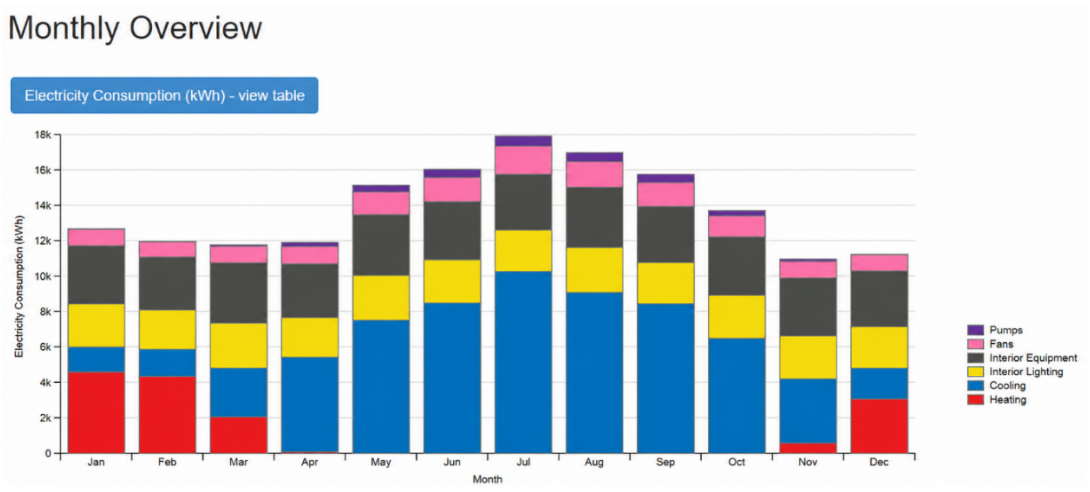


**Figure 10.** Annual energy consumption of Case 2.

### 3.1.3. VRF System (Case 3)

The VRF system was composed of 16 air-cooled CDUs, each connected to one or two indoor VRF fan-coil units. With this arrangement, cooling was provided through direct refrigerant expansion, while the refrigerant flow rate was adjusted according to the cooling demand. The energy consumption results for the VRF case are shown

in Figure 11. Among all end uses, cooling accounted for the largest share of energy consumption, reaching 131,289 kWh annually. This result can be explained by the climatic conditions in Kaohsiung, where hot and humid weather leads to a relatively high cooling load. By comparison, the annual heating demand was small, with energy consumption of only 8,253 kWh. This is because winter conditions are generally mild, so the VRF system requires heating operation in heat-pump mode only for a limited period. Fan energy reached 19,589 kWh per year, primarily due to the operation of multiple indoor fan-coil units serving different zones. The annual energy use for office equipment and interior lighting was 38,883 kWh and 28,706 kWh, respectively. These two end-use loads acted as internal heat sources and therefore increased the building's cooling demand. The simulation results showed no energy consumption for pumps, heat rejection, humidification, or supplementary refrigeration. This result is mainly related to the design of the VRF system, where cooling and heating are handled by refrigerant circulation instead of relying on a separate chilled-water system or additional refrigeration equipment. On a monthly basis, the energy use followed the expected seasonal trend, increasing during periods with higher cooling demand and remaining relatively low when heating or cooling loads were limited. Heating demand was highest in January at 2545.89 kWh and December at 1680.03 kWh, and was nearly zero from April to October. Cooling demand began to rise in March, reaching 5,392.42 kWh, and peaked in July at 20,965.11 kWh. Lighting and equipment energy remained almost constant throughout the year. Fan energy also stayed within a narrow range of 1525–1674 kWh per month, indicating relatively steady operation of the indoor units. Total monthly electricity consumption ranged from 11,020.36 kWh in December to 28,122.9 kWh in July, giving an annual total of 226,719.48 kWh. Cooling accounted for about 58% of the total energy use. The VRF system offered flexible zoning and part-load control, but its annual energy use remained closely related to the high cooling demand of the subtropical climate. For similar office buildings, VRF performance may therefore be improved by applying more refined control strategies or combining it with other system arrangements.

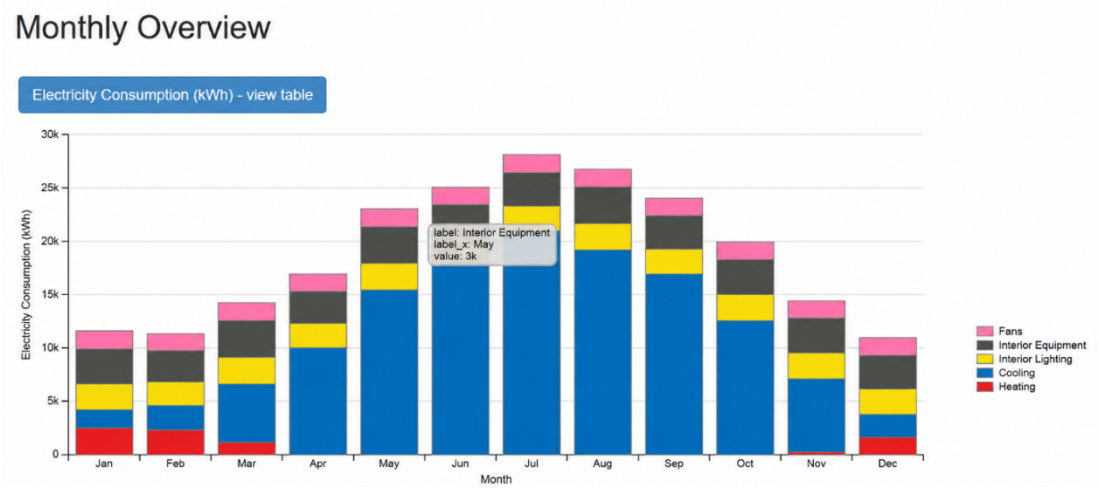


**Figure 11.** Annual energy consumption of Case 3.

### 3.1.4. FCU with Air-Cooled Chiller System (Case 4)

Case 4 used 27 four-pipe FCUs connected to separate chilled-water and hot-water loops. This arrangement allowed heating and cooling to be supplied at the same time according to the thermal demand of each zone. Since the studied building is located in a humid subtropical climate, where cooling is required for much of the year, this configuration was considered suitable for multi-zone office operation. The energy consumption results for the FCU system with an air-cooled chiller are shown in Figure 12. Cooling energy was the largest component of annual energy use, reaching 88,167 kWh. This reflects both the high cooling load of the building and the operation of the air-cooled chiller in maintaining indoor comfort. Heating energy was 19,831 kWh per year and was mainly related to hot-water loop operation during cooler periods. Fan and pump energy were 9219 kWh and 4294 kWh, respectively, corresponding to air circulation through the FCUs and water circulation in the chilled-water and hot-water loops. Office equipment and interior lighting consumed 38,883 kWh and 28,706 kWh per year, respectively, adding internal heat gains and increasing the cooling load. The monthly results followed the seasonal cooling demand. Cooling energy began to increase in March, reaching 3101.97 kWh, and peaked in July at 15,406.19 kWh. Cooling accounted for about 47% of the annual total energy consumption of 188,656 kWh. Heating demand was small on a monthly basis, while lighting and equipment loads remained nearly constant at about 2400 kWh and 3300 kWh per month, respectively. Fan and pump energy also increased during the cooling season, with

summer peak values of 1399.39 kWh and 645.18 kWh. Total monthly electricity consumption ranged from 7168.14 kWh in December to 22,948.65 kWh in July. The period from May to September accounted for 58% of the annual electricity use. The four-pipe FCU system provided flexible zone-level control and was suitable for spaces where simultaneous heating and cooling may be required. Compared with the VRF and VAV-DX systems, however, this configuration showed higher pump and heating energy use. Its performance could be further improved by using variable-speed drives, optimizing chiller operation under part-load conditions, and integrating renewable energy systems for subtropical office applications.

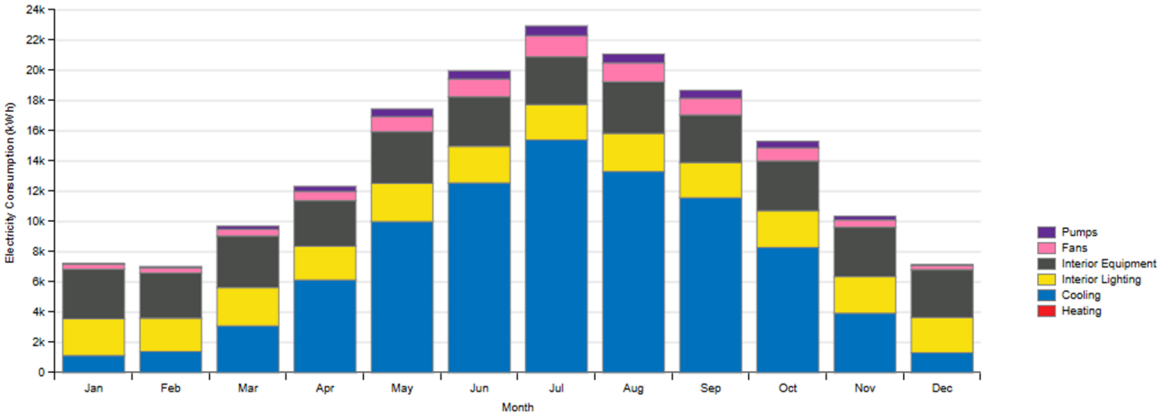


**Figure 12.** Annual energy consumption of Case 4.

The lower energy use of the VAV system with an air-cooled chiller is mainly related to its better part-load operation, more effective latent heat removal, and adjustable airflow control. In office buildings, HVAC systems often operate below full load for much of the time. During part-load operation, chiller-based systems tend to deliver more stable performance, while DX systems are more likely to lose efficiency because of repeated compressor cycling. In addition, humidity control is a key consideration in Taiwan, where the outdoor air is often warm and moisture-laden. The more stable coil temperature of chilled-water systems allows latent heat to be removed more effectively than in VRF or DX systems. As a result, indoor comfort can be improved with less additional energy required for humidity control. By comparison, the DX system showed the poorest performance because of its weaker part-load efficiency and limited dehumidification capacity. The VRF system provided zoning flexibility, but refrigerant distribution losses and control complexity may have reduced its overall efficiency. The FCU system also offered flexibility, although the additional pump energy and lack of centralized optimization led to only moderate energy performance.

### *3.2. Energy Use Intensity and Cost Analysis*

This study evaluates the energy performance of four HVAC system configurations implemented in a 2165 $m^2$ office building located in Kaohsiung, Taiwan, which is characterized by a hot and humid subtropical climate. The energy performance assessment was conducted in accordance with ASHRAE Standard 90.1-2019 [34]. The operating cost was calculated using the Taiwanese electricity tariff presented in Table 5. The tariff reference year used in this study was 2024. Electricity costs were converted from New Taiwan dollars (NTD) to USD using the average 2024 exchange rate of approximately 1 NTD = 0.031 USD. Table 6 summarizes the EUI and operating cost results for the four HVAC systems. Case 1 had the highest annual energy use, with an EUI of 41.59 kBtu/$ft^2$·yr and an annual consumption of 284,048 kWh. This value was higher than the ASHRAE Standard 90.1-2019 benchmark of 27.1 kBtu/$ft^2$·yr for small office buildings. The high energy use of Case 1 was mainly related to the limitations of DX cooling in hot climates and the relatively high energy demand of direct expansion operation. Case 2 had the lowest EUI among the four cases, at 24.322 kBtu/$ft^2$·yr, with an annual energy consumption of 166,106 kWh. This value met and slightly improved upon the ASHRAE benchmark. Compared with Case 1, Case 2 reduced annual energy consumption by 41.5%, showing the benefit of chiller-based cooling under subtropical climate conditions. Case 3 showed a middle-level result, with an EUI of 33.2 kBtu/$ft^2$·yr and annual energy consumption of 226,720 kWh. Although it used less energy than Case 1, it was still less efficient than the chiller-based configurations, which suggests that its suitability may be limited for office buildings of this scale in subtropical regions. Case 4 also showed favorable performance, with an EUI of 27.62 kBtu/$ft^2$·yr and annual energy consumption of 188,656 kWh. This value was close to the ASHRAE benchmark and represented a 33.6% reduction in energy consumption compared with Case 1. Taken together, the EUI results indicate that the chiller-

based systems performed better than the DX-based system under the hot and humid conditions considered in this study, regardless of the air distribution strategy.

The comparison confirms that HVAC system selection influenced the annual energy performance of the studied office building. Case 2 provided the highest energy efficiency among the four configurations, followed by Case 4 and Case 3. Case 1 showed the lowest efficiency. For subtropical office buildings, the selection of HVAC systems should therefore focus on cooling efficiency and annual energy consumption.

**Table 5.** Electricity tariff used for the operating cost calculation in Taiwan.

| | Peak/Off-Peak Time | | | Summer Electricity Rate (June 1st to September 30th) | Non-Summer Electricity Rate (Outside of Summer Months) |
|---|---|---|---|---|---|
| Basic electricity charge | Charged per household | | | 75.00 NTD/household | 75.00 NTD/household |
| Time-of-use electricity rate | Weekdays (Monday to Friday) | Peak hours | 09:00–24:00 (summer month) | 5.01 NTD/kWh | - |
| | | | 06:00–11:00<br>14:00–24:00<br>(not in summer months) | - | 4.78 NTD/kWh |
| | | Off-peak hours | 00:00–09:00 (summer month) | 1.96 NTD/kWh | - |
| | | | 00:00–06:00<br>11:00–14:00<br>(not in summer months) | - | 1.89 NTD/kWh |
| | Holidays (Saturday to Sunday) | Off-peak time | 00:00–24:00 | 1.96 NTD/kWh | 1.89 NTD/kWh |
| | Additional charge for monthly consumption exceeding 2000 kWh | | | +1.02 NTD/kWh | +1.02 NTD/kWh |

**Table 6.** Energy use intensity and cost comparison among the four HVAC system cases.

| Case | Energy Use Intensity (kBtu/ft$^2$·yr) | Total Cost (USD) |
|---|---|---|
| 1 | 41.59 | 43,033 |
| 2 | 24.32 | 23,971 |
| 3 | 33.20 | 34,336 |
| 4 | 27.62 | 25,672 |

### *3.3. Airflow and Temperature Distribution Results*

Figure 13 shows the CFD-simulated temperature field on the first floor at a height of 1 m. In the conditioned zones, the temperature was generally maintained between 24 and 25 °C, indicating a relatively uniform thermal distribution. The unconditioned areas were warmer because no HVAC conditioning was applied. These regions appeared as reddish–orange zones in the contour plot, with temperatures of approximately 27.5–31 °C. Figure 14 presents the airflow distribution on the same floor and at the same height. The simulated air velocity remained below 25 cm/s, which is within the commonly accepted comfort range and is unlikely to cause a draft sensation.

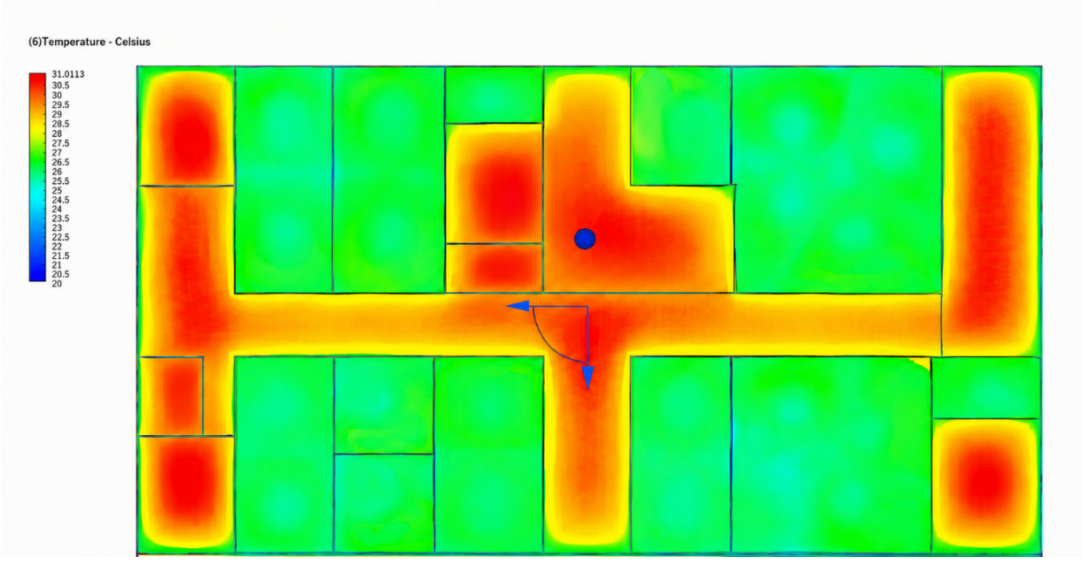


**Figure 13.** Temperature distribution on the first floor of the building.

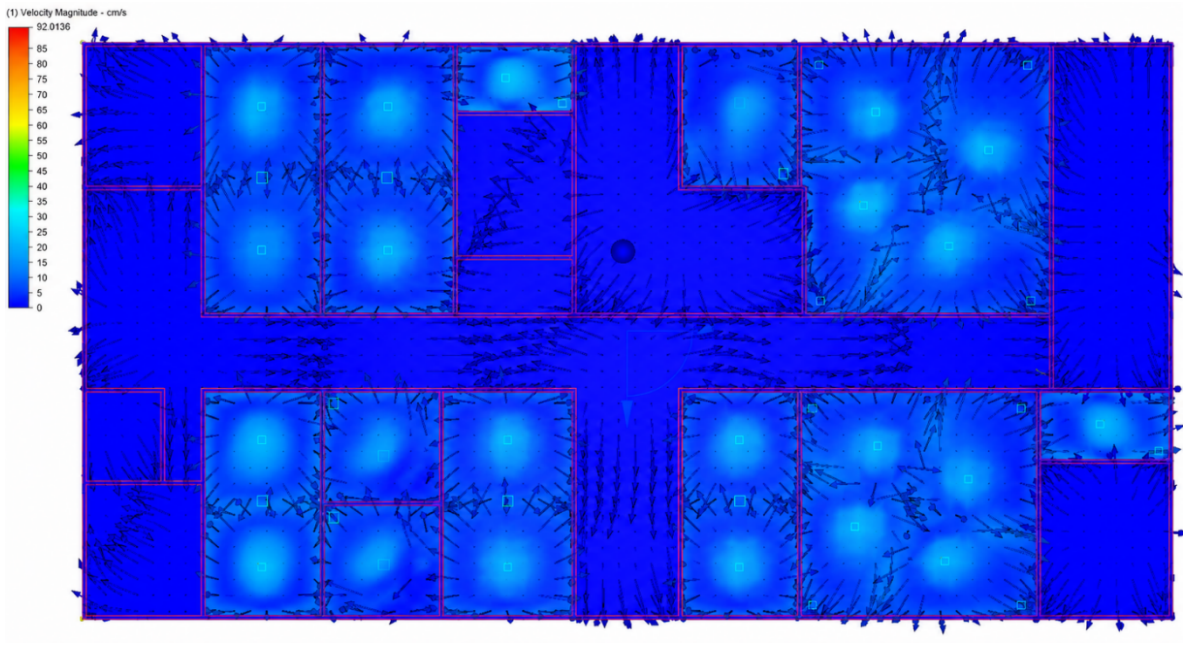


**Figure 14.** Flow distribution on the first floor of the building.

Figures 15 and 16 present the temperature and airflow distributions on the second floor. The conditioned zones maintained temperatures of approximately 24–25 °C, whereas the unconditioned zones were warmer, with temperatures ranging from 27.5 to 31 °C. The airflow field was examined on horizontal planes at a height of 1 m. The simulated air velocity remained below 20 cm/s, which is within the acceptable comfort range for office environments.

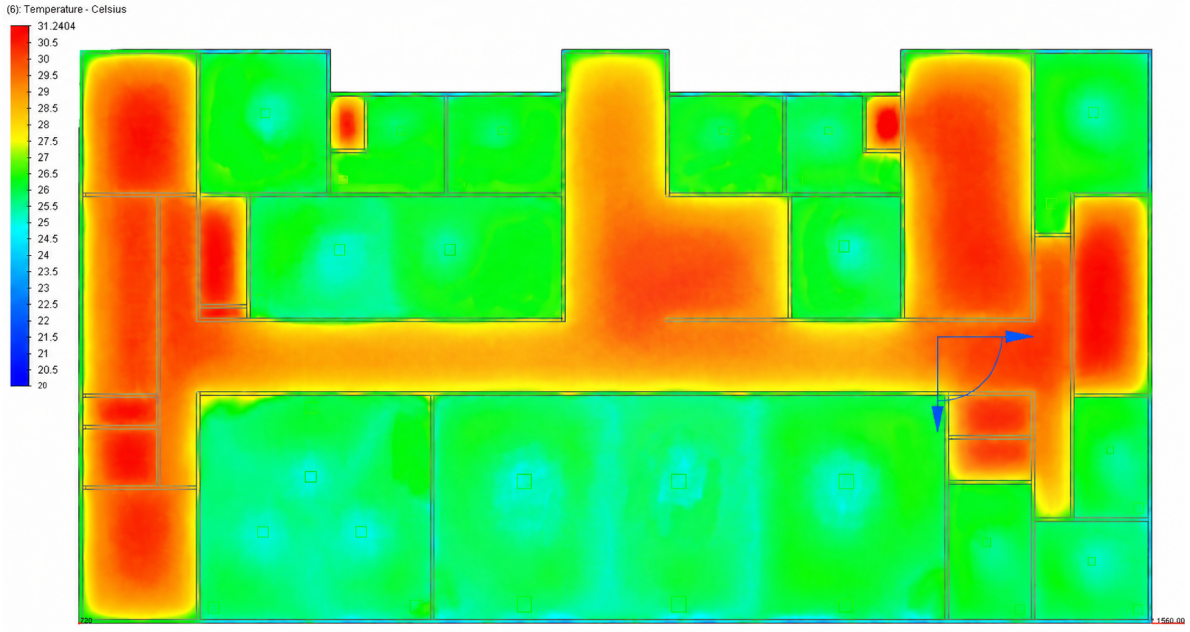


**Figure 15.** Temperature distribution on the second floor of the building.

In this study, CFD analysis was used to check the steady-state indoor airflow distribution and thermal comfort under the selected HVAC configurations. It was not used as the main basis for comparing system-level energy performance. On both the first and second floors, the simulated HVAC layouts maintained acceptable indoor thermal conditions in the occupied zones, with similar temperature ranges and airflow velocities. Therefore, the differences in energy consumption and EUI among the four cases were more closely related to HVAC system efficiency and cooling-source characteristics than to problems with air distribution or thermal comfort control.

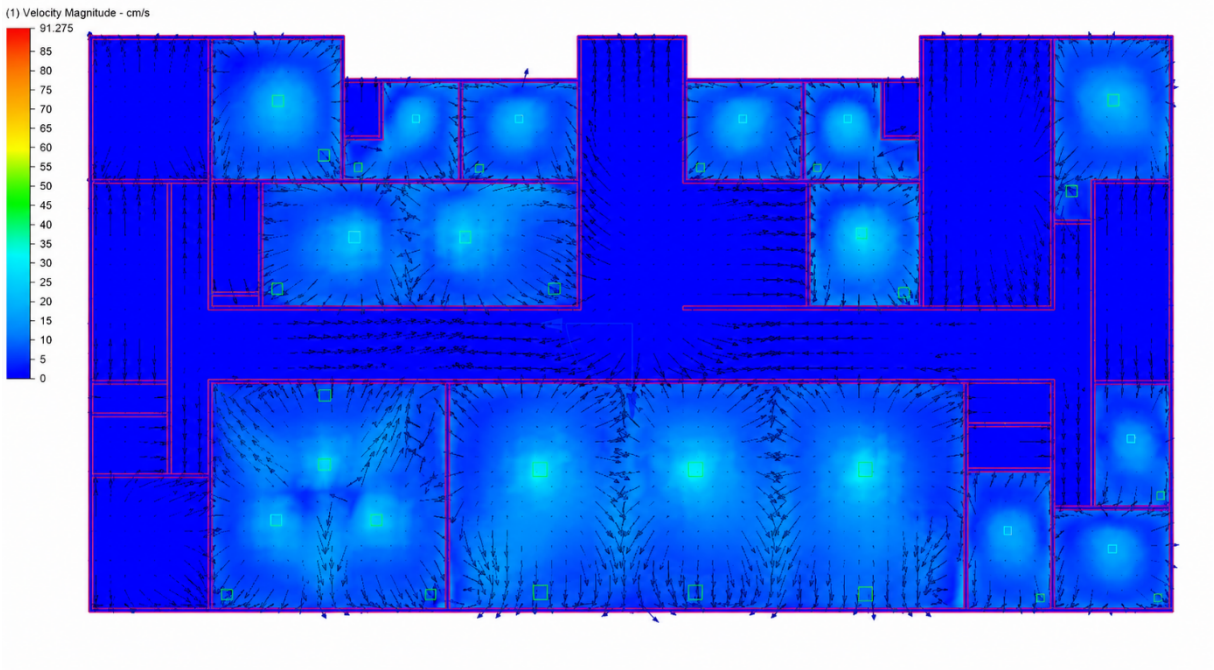


**Figure 16.** Flow distribution on the second floor of the building.

## 4. Conclusions

This work compared the energy performance and indoor thermal behavior of four HVAC configurations, referred to as Cases 1–4, for a 2165 m2 office building in Kaohsiung, Taiwan. All cases were analyzed using the same modeling assumptions under hot and humid subtropical climate conditions. The annual energy simulation results show that the choice of HVAC system affected the building energy performance under cooling-dominated operation. Among the four cases, Case 2 had the lowest EUI and the best energy performance. Case 4 also showed favorable results and may be useful for buildings that require functional flexibility or simultaneous heating and cooling. Case 3 presented intermediate energy performance, while Case 1 had the highest energy consumption, which may be related to lower part-load efficiency and the use of electric reheat. The CFD results showed that, under the prescribed boundary conditions, all four cases maintained acceptable airflow and temperature distributions in the occupied zones. For this building and the selected simulation conditions, the differences in annual energy use were therefore more closely related to system efficiency and cooling-source characteristics than to major differences in indoor air distribution. The results also indicate that chiller-based configurations, especially Case 2, may be more energy-efficient than the DX-based configuration for this office building in Kaohsiung. The results, however, should be interpreted within the limits of the present study, which considered only one building, one climate condition, one set of schedules and assumptions, and did not include field-based validation. Future work needs to include model calibration, sensitivity analysis, and additional building cases to examine whether the same trends apply more broadly.

**Author Contributions:** I.A.T.: investigation, data curation, writing—original draft; C.-K.W.: formal analysis, supervision, writing—review & editing; Y.-D.K.: conceptualization, methodology, supervision, writing—review & editing. All authors have read and agreed to the published version of the manuscript.

**Funding:** This research received no external funding.

**Institutional Review Board Statement:** Not applicable.

**Informed Consent Statement:** Not applicable.

**Data Availability Statement:** Not applicable.

**Conflicts of Interest:** The authors declare no conflict of interest.

**Use of AI and AI-Assisted Technologies:** During the preparation of this work, the authors used Grammarly for language polishing and grammar checking, and ChatGPT for assistance in creating the system schematic diagram. All data presented in this work are authentic experimental data and were not generated, modified, or fabricated by AI tools. After using these tools, the authors reviewed and edited the content as needed and take full responsibility for the published article.

## References


1. Liu, L.; Huang, Y. HVAC Design Optimization for Pharmaceutical Facilities with BIM and CFD. *Buildings* **2024**, *14*, 1627. https://doi.org/10.3390/buildings14061627.
2. Hong, D.; Cheng, R.; Lei, H.; et al. Comprehensive Review on the Impact of Building Envelopes on Indoor Thermal Comfort in Office Buildings: Balancing Occupant Comfort and Energy Efficiency. *Build. Environ.* **2026**, *289*, 114018. https://doi.org/10.1016/j.buildenv.2025.114018.
3. Huang, K.T.; Flowers, B. Parametric Optimisation of Building Envelopes for Energy Efficiency in Taiwan's Cooling-Dominated Climates. *Int. J. Sustain. Energy* **2025**, *44*, 2560863. https://doi.org/10.1080/14786451.2025.2560863.
4. Jang, E.; Heo, Y. A New Plenum-Based Dual-Mode Passive Cooling System Enabling Naturally Ventilated Core Zones in Office Buildings. *Build. Environ.* **2026**, *289*, 114026. https://doi.org/10.1016/j.buildenv.2025.114026.
5. Khdair, A.I.; Aburumman, G.A.; Tahmasbi, F.; et al. Advancing Natural Ventilation in Sustainable Architecture: Mechanisms, Innovations, and Climate-Responsive Design for Energy-Efficient Buildings. *Renew. Sustain. Energy Rev.* **2026**, *226*, 116314. https://doi.org/10.1016/j.rser.2025.116314.
6. Moharrami, M.; Sadeghifam, A.N.; Golzad, H.; et al. The Hybrid Attic Ventilation Technique as a Sustainable Strategy for Thermal Comfort Improvement and Energy Saving in Tropical Residential Buildings. *Energy Convers. Manag. X* **2025**, *26*, 100944. https://doi.org/10.1016/j.ecmx.2025.100944.
7. Gonzalez-Caceres, A.; Karlshøj, J.; Arvid Vik, T.; et al. Evaluation of Cost-Effective Measures for the Renovation of Existing Dwellings in the Framework of the Energy Certification System: A Case Study in Norway. *Energy Build.* **2022**, *264*, 112071. https://doi.org/10.1016/j.enbuild.2022.112071.
8. Ciccozzi, A.; Santavicca, A.; deRubeis, T.; et al. BIM-BEM Interoperability for Energy Analysis: A Comparative Study of Different Strategies. *Energy Rep.* **2025**, *13*, 4705–4718. https://doi.org/10.1016/j.egyr.2025.04.027.
9. Shalabi, F.; Turkan, Y. BIM-Energy Simulation Approach for Detecting Building Spaces with Faults and Problematic Behavior. *J. Inf. Technol. Constr.* **2020**, *25*, 342–360. https://doi.org/10.36680/J.ITCON.2020.020.
10. Al-Saeed, Y.W.; Ahmed, A. Evaluating Design Strategies for Nearly Zero Energy Buildings in the Middle East and North Africa Regions. *Designs* **2018**, *2*, 35. https://doi.org/10.3390/designs2040035.
11. Numan, M.; Saadat, U.; Farooq, M.U. BIM and Sustainable Design: A Review of Strategies and Tools for Green Building Practices. *J. Eng. Res. Sci.* **2024**, *3*, 1–7. https://doi.org/10.55708/js0302001.
12. Elnabawi, M.H. Building Information Modeling-Based Building Energy Modeling: Investigation of Interoperability and Simulation Results. *Front. Built Environ.* **2020**, *6*, 573971. https://doi.org/10.3389/fbuil.2020.573971.
13. Ahmed, W.; Heywood, C.; Holzer, D. BIM-Enabled Energy Retrofitting: A Critical Review of Current Status and Future Prospects. *Energy Build.* **2025**, *348*, 116478. https://doi.org/10.1016/j.enbuild.2025.116478.
14. Stegnar, G.; Cerovšek, T. Information Needs for Progressive BIM Methodology Supporting the Holistic Energy Renovation of Office Buildings. *Energy* **2019**, *173*, 317–331. https://doi.org/10.1016/j.energy.2019.02.087.
15. Veerendra, G.T.N.; Dey, S.; Mantle, E.J.; et al. Building Information Modeling—Simulation and Analysis of a University Edifice and Its Environs—A Sustainable Design Approach. *Green Technol. Sustain.* **2025**, *3*, 100150. https://doi.org/10.1016/j.grets.2024.100150.
16. Salem, E.; Elwakil, E. Optimizing Building Energy Performance Using BIM and Climate-Driven Site Data. *Innov. Infrastruct. Solut.* **2025**, *10*, 435. https://doi.org/10.1007/s41062-025-02221-5.
17. Hong, T.; Langevin, J.; Sun, K. Building Simulation: Ten Challenges. *Build. Simul.* **2018**, *11*, 871–898. https://doi.org/10.1007/s12273-018-0444-x.
18. Lin, K.L.; Jan, M.Y.; Liao, C. Sen. Energy Consumption Analysis for Concrete Residences—A Baseline Study in Taiwan. *Sustainability* **2017**, *9*, 257. https://doi.org/10.3390/su9020257.
19. Kang, K.Y.; Wang, X.; Wang, J.; et al. Utility of BIM-CFD Integration in the Design and Performance Analysis for Buildings and Infrastructures of Architecture, Engineering and Construction Industry. *Buildings* **2022**, *12*, 651. https://doi.org/10.3390/buildings12050651.
20. Albatayneh, A.; Alterman, D.; Page, A.W.; et al. Warming Issues Associated with the Long Term Simulation of Housing Using CFD Analysis. *J. Green Build.* **2016**, *11*, 57–74. https://doi.org/10.3992/jgb.11.2.57.1.
21. Liu, W.; Lian, S.; Fang, X.; et al. An Open-Source and Experimentally Guided CFD Strategy for Predicting Air Distribution in Data Centers with Air-Cooling. *Build. Environ.* **2023**, *242*, 110542. https://doi.org/10.1016/j.buildenv.2023.110542.
22. William, M.A.; Suárez-López, M.J.; Soutullo, S.; et al. Multi-Objective Integrated BES-CFD Co-Simulation Approach towards Pandemic Proof Buildings. *Energy Rep.* **2022**, *8*, 137–152. https://doi.org/10.1016/j.egyr.2022.06.091.
23. Ismail, N.; Ouahrani, D. A Comprehensive Optimization Study of Personal Cooling Radiant Desks Integrated to HVAC System for Energy Efficiency and Thermal Comfort in Office Buildings. *Int. J. Refrig.* **2023**, *156*, 54–71. https://doi.org/10.1016/j.ijrefrig.2023.09.023.

24. Mahecha Zambrano, J.; Baldini, L. Integrating CFD and Thermoregulation Models: A Novel Framework for Thermal Comfort Analysis of Non-Uniform Indoor Environments. *Energy Build.* **2025**, *335*, 115570. https://doi.org/10.1016/j.enbuild.2025.115570.
25. Chung, W.; Hui, Y.V.; Lam, Y.M. Benchmarking the Energy Efficiency of Commercial Buildings. *Appl. Energy* **2006**, *83*, 1–14. https://doi.org/10.1016/j.apenergy.2004.11.003.
26. Syarifudin, S.; Saputra, A.; Siswosukarto, S. An Analysis of Energy Consumption in the Campus Building's Operation (Case Study: The Building of Faculty of Engineering and Department of Civil and Environmental Engineering, Universitas Gadjah Mada). *J. Civ. Eng. Forum* **2018**, *4*, 67–78. https://doi.org/10.22146/jcef.27642.
27. Mogili, S.; Avvari, H.V.; Appecharla, V.K. Energy Consumption Analysis of Residential Building Using Autodesk Revit. *IOP Conf. Ser. Earth Environ. Sci.* **2022**, *1086*, 012056. https://doi.org/10.1088/1755-1315/1086/1/012056.
28. Dwivedi, E.; Kashyap, R.; Kumar, R.R. Evaluating the Effectiveness of Energy-Efficient Design Strategies in Achieving Net Zero Energy Building through Reduced Energy Consumption. *Int. J. Res. Appl. Sci. Eng. Technol.* **2023**, *11*, 1766–1779. https://doi.org/10.22214/ijraset.2023.49774.
29. Akhilesh, U.S.; George, D.G. Energy Analysis & Optimization of a Residential Structure. *Int. J. Sci. Res. Eng. Manag.* **2024**, *8*. https://doi.org/10.55041/ijsrem37231.
30. Raftery, P.; Li, S.; Jin, B.; et al. Evaluation of a Cost-Responsive Supply Air Temperature Reset Strategy in an Office Building. *Energy Build.* **2018**, *158*, 356–370. https://doi.org/10.1016/j.enbuild.2017.10.017.
31. Muta, L.F.; Melo, A.P.; Lamberts, R. Enhancing Energy Performance Assessment and Labeling in Buildings: A Review of BIM-Based Approaches. *J. Build. Eng.* **2025**, *103*, 112089. https://doi.org/10.1016/j.jobe.2025.112089.
32. Kulthanaphanich, Y.; Permata, R.; Lin, S.Y. Life Cycle Assessment of Integrated Energy and Seismic Retrofits for Existing Buildings. *J. Build. Eng.* **2025**, *108*, 112967. https://doi.org/10.1016/j.jobe.2025.112967.
33. Taheri, S.; Norouzijajarm, E.; Athar, A.A. Technical, Economic, and Environmental Assessment of Energy Audit and Optimization in the Mechanical Room of an Office Building. *Energy Sustain. Dev.* **2025**, *87*, 101717. https://doi.org/10.1016/j.esd.2025.101717.
34. U.S. Department of Energy. *Preliminary Energy Savings Analysis: ANSI/ASHRAE/IES Standard 90.1-2019*; U.S. Department of Energy: Washington, DC, USA, 2021.
35. Nambiar, C.; Hart, R.; Rosenberg, M.; et al. End Use Analysis of ANSI/ASHRAE/IES Standard 90.1-2019. *ASHRAE J.* **2023**, *65*, 34–42.